CHALLENGES IN EUROPEAN AEROSPACE
5TH CEAS AIR & SPACE CONFERENCE

CEAS

Use of Simulator Motion Feedback for Different Classes of Vehicle Dynamics in Manual Control Tasks

T. Lu
Control and Simulation Section, Faculty of Aerospace Engineering, Delft University of Technology
PhD student
Kluyverweg 1, 2629HS, Delft, Holland, the Netherlands
T.Lu-3@tudelft.nl
D. M. Pool (Control and Simulation Division, Faculty of Aerospace Engineering, Delft University of Technology), M. M. van Paassen (Control and Simulation Division, Faculty of Aerospace Engineering, Delft University of Technology), M. Mulder (Control and Simulation Division, Faculty of Aerospace Engineering, Delft University of Technology)

ABSTRACT

With the development of moving-based flight simulators in mind, a large number of researchers have considered human manual control behavior in tasks where the motion of the controlled vehicle can be felt by the pilots. While it is known that the dynamics of the controlled vehicle are a key factor that determines the usefulness of motion feedback, there is no systematic study of the use of motion feedback over a wide range of controlled dynamics. Therefore, this paper describes a human-in-the-loop yaw attitude compensatory tracking experiment that was conducted to evaluate the effects of motion feedback on task performance, as well as the open-loop crossover frequency and phase margin. A gain, a single integrator and a double integrator were selected as the different controlled elements in this experiment, respectively. For the double integrator controlled element, the results confirms the findings of previous studies that the motion feedback is crucial in improving task performance and increasing the open-loop phase margin for enhanced stability. However, for both the gain and single integrator controlled elements, the motion feedback is not helpful in the aspect of changing task performance, target crossover frequency and phase margin.

1 INTRODUCTION

Nowadays, aircraft flight simulators are widely used in the aviation industry to train pilots. Furthermore, most advanced flight simulators are moving-base devices, which can provide pilots with a physical sensation of the motion of their aircraft. However, in manual control tasks, it is well-known that pilots change their control strategies according to numerous internal and external factors [1], one of the most dominant is the dynamics of the controlled element. According to McRuer et al. [1], pilots adapt their own control dynamics to those of the controlled system to achieve the best task performance without destabilizing the closed-loop system. Based on the characteristics of different controlled elements, the corresponding task performance, bandwidth of manual control and the stability of the closed-loop system may differ greatly. Another important factor affecting pilot control is physical motion feedback, which pilots can utilize to improve their task performance and decrease their crossover frequency while retaining adequate stability of the closed-loop system [2, 3].

Whether motion feedback is always beneficial (to improve task performance, decrease crossover frequency and/or improve the stability of the closed-loop system) is not yet fully clear, especially with

respect to different types of control tasks, such as position control, velocity control and acceleration control. In numerous studies, it has been proven that for control of marginally stable dynamics like a double integrator (acceleration control), motion feedback is beneficial [4, 5, 6, 7, 8]. The underlying mechanism is that the motion feedback is utilized to help pilot generate lead and stabilize the system. For more inherently stable controlled elements such as a single integrator (velocity control), the conclusions about the usefulness of motion feedback are much less consistent. For example, Bergeron [9] found no change in task performance when motion feedback was added. However, Stapleford et al. [5] reported that with motion feedback better task performance, as well as higher crossover frequency and phase lead were observed.

For even more stable controlled elements, like gain dynamics (position control), the effect of motion feedback is also not fully clear. Early studies agreed that for this kind of controlled element, the motion feedback is not helpful in improving task performance, decreasing the crossover frequency or increasing the stability of the closed-loop system, since the information that may be obtained from the physical motion feedback is not needed [4, 10]. However, as Junker et al. [11] reported, the motion feedback may still negatively affect pilots during manual control, so it is still important to verify which kind (no influence or negative) and to what an extent motion feedback may affect pilots during gain control tasks.

To investigate the effects of physical motion feedback on manual control tasks with different controlled elements, a human-in-the-loop yaw attitude compensatory tracking experiment was carried out in the SIMNONA Research Simulator in Delft University of Technology. To cover a wide range of controlled elements, a gain, a single integrator and a double integrator controlled element (representing positon, velocity and acceleration controls) were evaluated in this experiment both with and without motion feedback, respectively. Task performance was calculated by the variance of the tracking error. The target-to-error and disturbance-to-error frequency response functions calculated using both estimated frequency response function [12] and multimodal pilot modeling techniques [13] are used to further analyze the origins of measured differences in task performance. The target open-loop crossover frequency and phase margin are calculated as the indications of pilot manual control bandwidth and stability of the closed-loop system.

The structure of this paper is as follows. In Section 2 the details of the yaw attitude tracking experiment and corresponding data analysis methods are introduced. Then in Section 3 the results of the human-in-the-loop experiment are presented. The paper ends with a discussion and conclusions.

2 METHODS

2.1 Control Task

In the experiment, a yaw attitude tracking task was used to evaluate the effects of motion feedback on tracking performance, target crossover frequency and phase margin with different controlled elements. A block diagram representation of this control task is shown in **Figure 1**. Pilots were asked to control the yaw angle ψ of the controlled element H_c by tracking the target signal f_t to minimize the error signal e shown on a compensatory display (**Figure 2**). The physical motion feedback of the controlled element yaw angle ψ is available to the pilot when the motion system of the simulator is active, shown with the dashed lines. In addition, the control task includes disturbance signal f_d. In **Figure 1**, H_{pe} represents the pilot's visual channel, processing the error signal e observed from the compensatory display and

$H_{p\psi}$ represents the pilot's motion channel, processing the motion feedback signal ψ provided by the motion system of the simulator. The details of H_{pe} and $H_{p\psi}$ are not considered in the current paper, but can be found in [14].

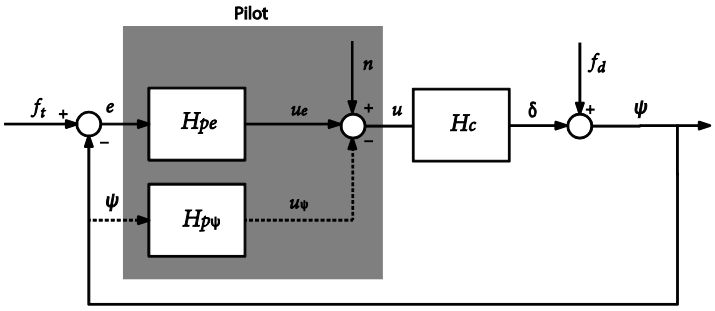

Figure 1: The closed-loop yaw attitude tracking task.

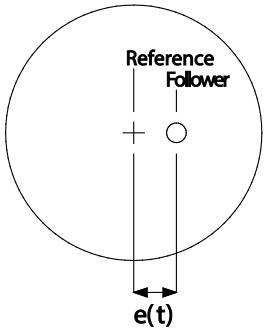

Figure 2: Compensatory display.

2.2 Controlled Element Dynamics

The controlled elements H_c used in the yaw attitude tracking task (see **Figure 1**) are given as:

$$H_{c,g} = \frac{1}{(\frac{1}{10}s+1)^2(\frac{1}{30}s+1)} \approx 1 \quad (1)$$

$$H_{c,si} = \frac{4}{s(\frac{1}{30}s+1)^2} \approx \frac{4}{s} \quad (2)$$

$$H_{c,di} = \frac{15}{s^2} \quad (3)$$

The first controlled element, Eq. (1), within the human manual control bandwidth, which ranges from 2 rad/s to 5 rad/s [1], approximates a pure unity gain. For practical reasons, i.e. to be able to compute the yaw acceleration $\ddot{\psi}$ needed for driving the SIMONA Research Simulator motion system and suppress the motion at high frequencies, two break frequencies (10 rad/s and 30 rad/s) are added in the denominator. The second controlled element, Eq. (2) approximates a single integrator within the human manual control bandwidth. The denominator with break frequency 30 rad/s is added for the same reason of the gain-like controlled element. The third controlled element, Eq. (3), is a pure double integrator. For convenience, in the remainder of this paper, Eq. (1), Eq. (2) and Eq. (3) are referred to as gain, single integrator and double integrator controlled elements, respectively.

2.3 Forcing Functions

In order to identify the pilot's visual channel H_{pe} and motion channel $H_{p\psi}$, both the target and disturbance signals shown in **Figure 1** are chosen to be the sums of 10 sine waves with independent frequencies, as given by:

$$f_{t,d}(t) = \sum_{k=1}^{10} A_{t,d}(k) sin[\omega_{t,d}(k)t + \phi_{t,d}(k)] \tag{4}$$

where $A_{t,d}(k)$, $\omega_{t,d}(k)$ and $\phi_{t,d}(k)$ are the amplitude, frequency and phase of the kth sine wave in the target forcing function f_t and disturbance forcing function f_d, respectively.

For both forcing functions the amplitude distribution [15] makes the control task realistic and not too difficult. Meanwhile, the amplitude distribution ensures that the control task is primarily a target tracking task. The experimental measurement time of a tracking run was 81.92 s, thus the base frequency is $\omega_m = 2\pi / 81.92 \text{ s} = 0.077$ rad/s. To avoid spectral leakage, the frequency of each sine wave component was defined as an integer multiple of the base frequency $\omega_{t,d} = n_{t,d}\omega_m$, the integer factors are shown in **Table 1**, respectively. The phases ϕ_t and ϕ_d were selected to yield signals with an approximately Gaussian distribution and without excessive peaks [16].

Table 1: Target and disturbance forcing function parameters.

	f_t				f_d			
k	n_t	ω_t,rad/s	A_t,deg	ϕ_t,rad	n_d	ω_d,rad/s	A_d,deg	ϕ_d,rad
1	6	0.460	4.277	1.288	5	0.383	2.057	-0.269
2	13	0.997	2.991	6.089	11	0.844	1.555	4.016
3	27	2.071	1.350	5.507	23	1.764	0.775	-0.806
4	41	3.145	0.727	1.734	37	2.838	0.395	4.938
5	53	4.065	0.488	2.019	51	3.912	0.240	5.442
6	73	5.599	0.302	0.441	71	5.446	0.146	2.274
7	103	7.900	0.192	5.175	101	7.747	0.091	1.636
8	139	10.661	0.140	3.415	137	10.508	0.066	2.973
9	194	14.880	0.109	1.066	171	13.116	0.055	3.429
10	229	17.564	0.100	3.479	226	17.334	0.047	3.486

2.4 Independent Variables

In order to reveal the effects of motion feedback on tracking performance and the target open-loop crossover frequency and phase margin with different controlled elements, the experiment had a full-factorial design with two independent variables. This means that all combinations of the motion feedback on/off and the three different controlled elements were evaluated, see **Table 2**:

Table 2: Experimental conditions.

Controlled element	Motion off	Motion on
Gain, $H_{c,g}$	C1	C4
Single integrator, $H_{c,si}$	C2	C5
Double integrator, $H_{c,di}$	C3	C6

2.5 Target-to-Error and Disturbance-to-Error Frequency response functions

In order to further compare how the tracking of f_t and the rejection of f_d are affected by the presence of motion feedback, the frequency response function between error signal e and target forcing function f_t is estimated from the measured data according to:

$$\hat{H}_{e,f_t}(j\omega_t) = \frac{E(j\omega_t)}{FT(j\omega_t)} \tag{5}$$

where $E(j\omega_t)$ is the Fourier transform of the measured error signal e at frequency set of ω_t, $FT(j\omega_t)$ is the Fourier transform of the target forcing function f_t at frequency set of ω_t. Similarly, the frequency response function between the error signal e and the disturbance forcing function f_d can be derived as:

$$\hat{H}_{e,f_d}(j\omega_d) = \frac{E(j\omega_d)}{FD(j\omega_d)} \tag{6}$$

where $E(j\omega_d)$ is the Fourier transform of the error signal e at frequency set of ω_d, $FD(j\omega_d)$ is the Fourier transform of disturbance forcing function f_d at frequency set ω_d.

In order to better analyse the continuous changing trends of target-to-error and disturbance-to-error dynamics and to observe its fitting with the discrete frequency response functions (Eq. (5), Eq. (6)), the continuous frequency response functions are derived:

$$H_{e,f_t}(j\omega) = \frac{1 + H_{p\psi}(j\omega)H_c(j\omega)}{1 + [H_{pe}(j\omega) + H_{p\psi}(j\omega)]H_c(j\omega)} \tag{7}$$

$$H_{e,f_d}(j\omega) = \frac{-H_c(j\omega)}{1 + [H_{pe}(j\omega) + H_{p\psi}(j\omega)]H_c(j\omega)} \tag{8}$$

For the no motion conditions, $H_{p\psi} = 0$. The details of H_{pe} and $H_{p\psi}$ can be found in [14].

The frequency response functions derived above describe in the frequency domain how the target signal and disturbance signal transfer into the error signal and thus affect overall task performance. In a manual control task, the pilot can only suppress the target or disturbance signal below a certain frequency, which is usually around the open-loop crossover frequency. Just above this frequency, the magnitude of the closed-loop responses will show a distinct peak, indicating that the errors induced by the target and disturbance signals are amplified, a result of the inherent delay in the human pilot [1]. In general, a high crossover frequency corresponds with a better low-frequency error attenuation, but with a stronger error amplification at higher frequencies. In control theory, the more pronounced the closed-loop system peak, the lower the stability of the closed-loop system, which corresponds with a lower open-loop phase margin.

2.6 Dependent Variables and Data Analysis

During each run of the experiment, the measured variables include the time histories of the tracking error e, the pilot control input u and controlled element yaw angle ψ (see **Figure 1**). For the data analysis, the variance of e is calculated as the tracking performance, Fourier coefficient method [12] and multimodal pilot modelling techniques [13] are used to calculate the target-to-error and disturbance-to-error frequency response functions, and the target open-loop crossover frequency and phase margin are calculated as indications for the manual control bandwidth and the stability of the closed-loop system. A repeated-measures analysis of variance (ANOVA) is done to reveal any significant effect of the independent variables on the error variance, target crossover frequency and phase margin. A repeated t-test is further used to judge the significance of observed effects of motion feedback for each controlled element individually.

2.7 Apparatus and Subjects

The experiment was performed in the SIMONA Research Simulator of Delft University of Technology. The subjects were seated in the right pilot seat in the cabin and a sidestick was used for giving control inputs. The compensatory display (**Figure 2**) was presented on the primary flight display (PFD) directly in front of the subjects. For C4, C5 and C6, the yaw motion cues around a subject's vertical axis were provided through the simulator motion system. For all conditions including the no motion conditions C1, C2 and C3, a noise-cancelling headset was used to prevent subjects hearing the noise produced by the simulator actuators.

Figure 3: The SIMONA Research Simulator.

Six subjects (aged from 25 to 53) for this experiment were students and staff of the Faculty of Aerospace Engineering of Delft University of Technology. All subjects had experience with similar manual control tasks from previous human-in-the-loop experiments. Each subject received an experimental briefing on the overview and objective of the experiment and gave the written informed consent before the start of the experiment. The experimental conditions (**Table 2**) were known to all subjects. The subjects were instructed to minimize the yaw attitude tracking error e presented on the PFD as best as possible.

3 RESULTS

In this section the results of the human-in-the-loop experiment are presented. The measured tracking performance is discussed first. Then the results of target open-loop crossover frequency and phase margin are provided. Finally, the measured frequency responses of the target-to-error and disturbance-to-error dynamics are analysed.

3.1 Tracking Performance

Figure 4 shows the measured variance of the error signal e for each condition, averaged over the six subjects. The error bars show the average and 95% confidence interval of the mean total $\sigma^2(e)$. The data have been corrected for between-subject variability. As can be seen in **Figure 4**, there is no obvious difference in $\sigma^2(e)$ between C1 and C4, which suggests that motion feedback is not helpful in improving tracking performance for the pure gain controlled element. For the single integrator, there is a slight increase in the average $\sigma^2(e)$ in C5 compared to C2, meaning slightly worse tracking performance with motion. For the double integrator, an improvement in tracking performance can be clearly observed when motion feedback is added in C6. Since the double integrator is most difficult to control, $\sigma^2(e)$ for C3 and C6 is markedly higher than for the other conditions. It can be verified from **Table 3** that both the controlled element H_c ($F(2,10)=32.7$, $p<0.05$) and the motion Mot ($F(1,5)=21.6$, $p<0.05$) significantly affect $\sigma^2(e)$. To further illustrate the effect of motion on each controlled element, the horizontal bars in **Figure 4** show the results of a dependent t-test performed between C1 and C4, C2 and C5, C3 and C6, respectively, where "-" means no significant difference and "*" means significant difference. As can be seen, only the difference of $\sigma^2(e)$ between C3 and C6, is significant.

Figure 4 also shows the contributions of the target forcing function, the disturbance forcing function and the pilot-induced noise to the total tracking error variances, marked with the different coloured portions of each bar. As can be seen for all conditions, the variance component of the target forcing function is the main contributor to the total variance, due to the fact that the control task of the experiment is primarily a target tracking task. In **Table 3** it can be observed that the error variance attributed to the target signal, $\sigma^2(e, f_t)$ ($F(1,5)=7.8$, $p<0.05$), and the disturbance signal, $\sigma^2(e, f_d)$ ($F(1,5)=17.6$, $p<0.05$), both seem to vary significantly with the presence of motion feedback (Mot). For example, in **Figure 4,** with the added motion, the target component of C5 is higher than that of C2, and the target component of C6 is much lower than that of C3. For the disturbance component, the difference between C3 and C6 is obvious, but for the gain and single integrator, the disturbance components are almost identical between conditions with and without motion.

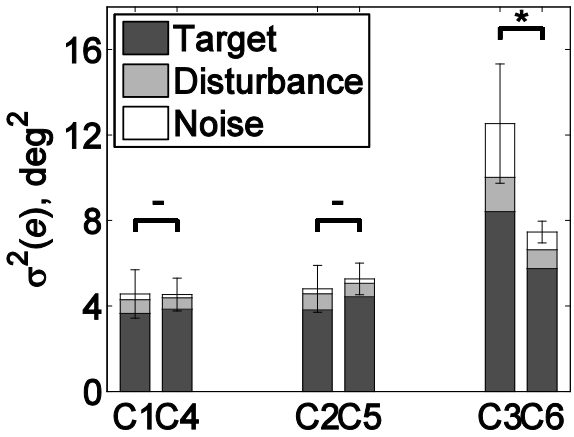

Figure 4: Variance of the error signal for each condition.

Table 3: ANOVA results of error variance $\sigma^2(e)$ and its components, where * is significant ($p < 0.05$), and - is not significant ($p \geq 0.05$).

	$\sigma^2(e)$			$\sigma^2(e, f_t)$			$\sigma^2(e, f_d)$		
Factor	df	F	Sig.	df	F	Sig.	df	F	Sig.
H_c	2,10	32.7	*	2,10	21.5	*	2,10	22.2	*
Mot	1,5	21.6	*	1,5	7.8	*	1,5	17.6	*
$H_c \times Mot$	2,10	19.5	*	2,10	16	*	2,10	6.4	*

3.2 Target Crossover Frequency and Target Phase Margin

Figure 5 shows error-bar plots of the measured target open-loop crossover frequencies $\omega_{c,t}$ and target phase margins $\phi_{m,t}$ for all conditions. The error bars show the average and 95% confidence interval of the means over six subjects, and the data have been corrected for between-subject variability. It can be seen in **Figure 5(a)** that there is no obvious difference of $\omega_{c,t}$ between C1 and C4, which indicates that the motion may not cause target crossover frequency difference for the gain control tasks. For the single integrator, the average $\omega_{c,t}$ of C5 is somewhat lower than that found for C2, meaning that the motion may help decrease the target crossover frequency for single integrator control task in average. The average $\omega_{c,t}$ for C6 is lower than that for C3, indicating that the motion decreases the target crossover frequency for the double integrator control task. However, in **Table 4**, the controlled element H_c is the only independent variable having significant effect on $\omega_{c,t}$ ($F(2,10) = 5.2$, $p < 0.05$). To individually analyse the motion effects on different controlled elements, **Figure 5(a)** also shows the dependent t-test results of $\omega_{c,t}$, showing only for the double integrator, the motion effect is significant.

In **Figure 5(b)**, for the gain controlled element, a slight decrease of the average target phase margin $\phi_{m,t}$ in C4 compared with C1 can be observed, suggesting that the closed-loop stability of C4 is lower than that of C1. For the single integrator controlled element, there is no obvious difference in $\phi_{m,t}$ between C2 and C5, indicating that the motion does not affect the closed-loop stability in single integrator control tasks. For the double integrator controlled element, the average $\phi_{m,t}$ of C6 is much higher than that of C3, indicating a marked increase of the closed-loop system stability when motion is present. Since the gain controlled element is very stable, on average, $\phi_{m,t}$ of C1 and C4 is the highest among all the conditions, and this can be verified from **Table 4** that the effect of the controlled element H_c on $\phi_{m,t}$ is significant ($F(2,10)=87.6$, $p<0.05$). The interaction between the controlled element and the motion $H_c \times Mot$ is also found to be significant for $\phi_{m,t}$ ($F(2,10)=15$, $p<0.05$), caused by the difference in C1 and C4, no difference between C2 and C5, and the difference between C3 and C6 in **Figure 5(b)**. Additionally, the t-test results of $\phi_{m,t}$ show that only for the double integrator, the motion effect is significant.

Since this experiment is primarily a tracking task and the goal of this paper is to study the tracking performance, the disturbance crossover frequency and phase margin are not further analysed.

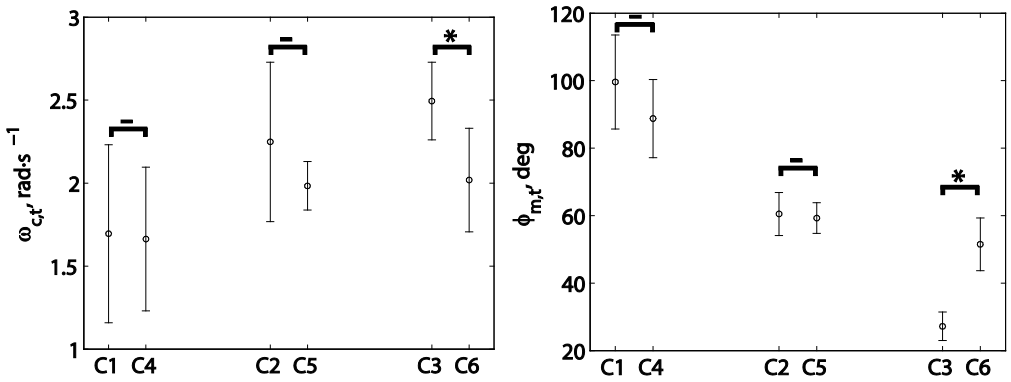

(a) Target crossover frequency (b) Target phase margin

Figure 5: Target crossover frequency and target phase margin for each condition.

Table 4: ANOVA results of target crossover frequency and target phase margin, where * is significant ($p<0.05$), and - is not significant ($p\geq 0.05$).

	$\omega_{c,t}$			$\phi_{m,t}$		
Factor	df	F	Sig.	df	F	Sig.
H_c	2,10	5.2	*	2,10	87.6	*
Mot	1,5	6.1	-	1,5	3.6	-
$H_c \times Mot$	2,10	1.2	-	2,10	15.0	*

3.3 Analysis of Closed-Loop Attenuation of Tracking Errors

Figure 6 shows the results of the closed-loop attenuation of tracking errors with respect to both the target (a-c) and disturbance (d-f) forcing functions of the three controlled elements. The error bars with triangles and circles represent the averages and 95% confidence intervals of the magnitude of the discrete frequency response function $H_{e,\,ft}$ (or $H_{e,\,fd}$) estimated using Eq. (5) (or Eq. (6)) for all subjects for the no-motion and motion conditions, respectively. The dashed and solid curves represent the magnitude of $H_{e,\,ft}$ (or $H_{e,\,fd}$) of the averaged subject calculated by Eq. (7) (or Eq. (8)) for no-motion and motion conditions, respectively. Finally, the dashed and solid vertical lines mark the target (or disturbance) crossover frequencies of the average pilot-vehicle system for both conditions, respectively. It can be seen that attenuation of the tracking errors induced by both forcing function signals, for which $\left|H_{e,\,ft}(j\omega)\right|<1$ (or $\left|H_{e,\,fd}(j\omega)\right|<1$), is only achieved below a certain frequency. For higher frequencies, the magnitude of the closed-loop responses overshoots and forms a peak, the height of which corresponds with the stability of the closed-loop system. As can be seen, the discrete frequency responses derived from Eq. (5) (or Eq. (6)) match well with the continuous ones derived from Eq. (7) (or Eq. (8)) in each plot.

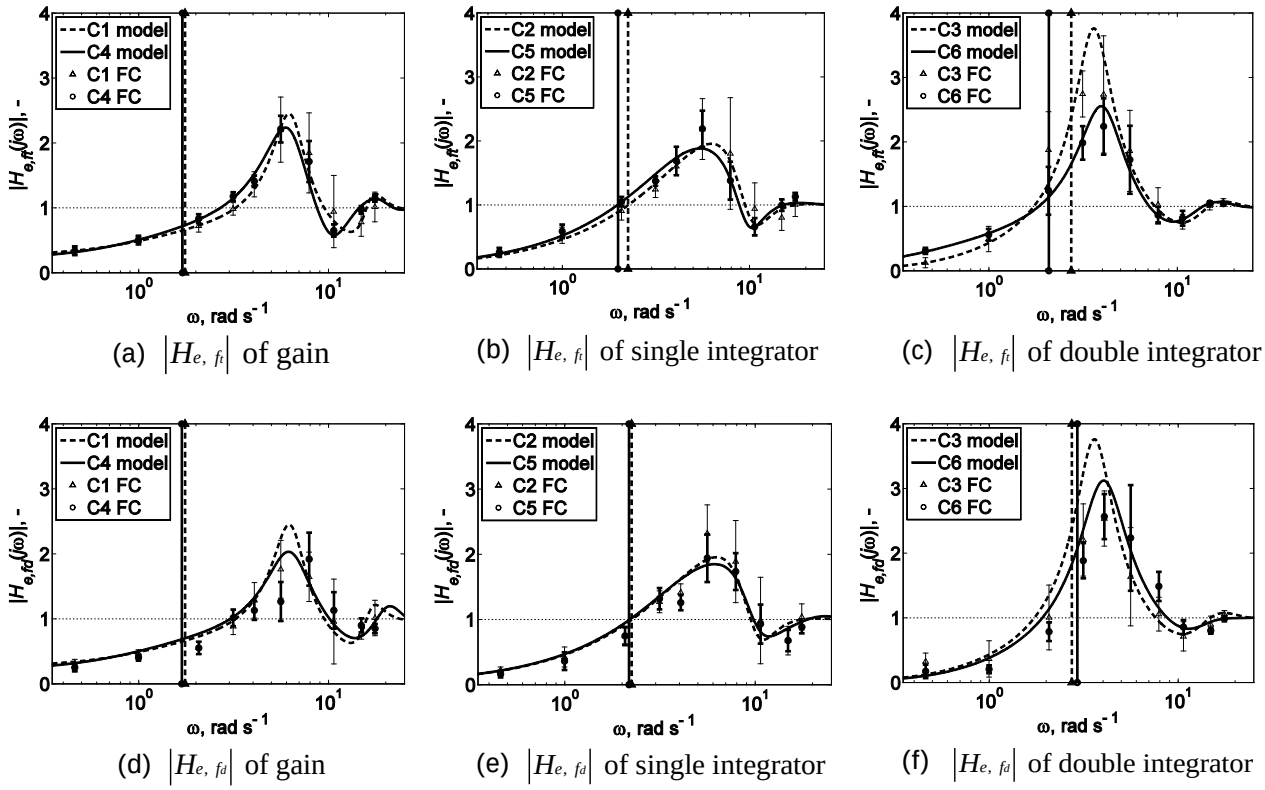

(a) $\left|H_{e,\,ft}\right|$ of gain (b) $\left|H_{e,\,ft}\right|$ of single integrator (c) $\left|H_{e,\,ft}\right|$ of double integrator

(d) $\left|H_{e,\,fd}\right|$ of gain (e) $\left|H_{e,\,fd}\right|$ of single integrator (f) $\left|H_{e,\,fd}\right|$ of double integrator

Figure 6: Frequency responses of target-to-error and disturbance-to-error dynamics.

In **Figure 6(c)** (and **Figure 6(f)**), obvious differences between the dashed and solid curves can be observed, especially around the frequencies of the peak. In **Figure 6(c)**, the peak of C6 is much lower than that of C3, indicating that the closed-loop system becomes more stable when motion feedback is

provided, and this accounts for the better performance of C6 than C3 observed in **Figure 4**. The lower target crossover frequency for C6 than for C3 (also see **Figure 5(a)**) is seen to result in slightly worse error attenuation at low frequencies, but result in a coupled significant reduction in the peak magnitude. In **Figure 6(f)**, even though the difference of the peaks between C3 and C6 is not as large as the one of **Figure 6(c)**, it still seems evident here in comparison with the results for the other controlled elements. The lowering of the closed-loop resonance peak between C3 and C6 in both **Figure 6(c)** and **Figure 6(f)** strongly influence the target and disturbance components of $\sigma^2(e)$, as presented in **Figure 4**, and causes both the target and disturbance components of C6 to be lower than those of C3.

Compared with the double integrator, in **Figure 6(a)** (and **Figure 6(d)**), the dashed and solid curves show much less difference, which indicates that for the gain control tasks, the error signal attenuation does not change much as a result of motion feedback. This is consistent with **Figure 4**, where the target and disturbance components for C1 nearly equal to those for C4. Furthermore, the nearly identical dashed and solid vertical lines in both **Figure 6(a)** and **Figure 6(d)** show that the target crossover frequencies of C1 and C4 are almost the same, and the disturbance crossover frequencies of C1 and C4 approximately equal as well. All observations from **Figure 6(a)** and **Figure 6(d)** indicate that for the gain controlled element the motion feedback is not helpful in improving task performance and decreasing crossover frequency.

In **Figure 6(b)**, compared with the dashed curve, the solid curve slightly shifts to the left, meaning that for frequencies below the peak, the error attenuation becomes marginally worse. As can be seen in **Figure 4**, the target component of $\sigma^2(e)$ of C5 is also slightly higher than for C2. Meanwhile, in **Figure 6(b)**, the target crossover frequency of C5 is lower than that of C2, and this difference is more obvious than that of the gain controlled element in **Figure 6(a)**. In **Figure 6(e),** the nearly identical dashed and solid curves indicate that the performance with respect to the disturbance forcing function are nearly identical as well, which is consistent with **Figure 4** where the disturbance components of $\sigma^2(e)$ for C2 and C5 are seen to be almost equal. **Figure 6(b)** and **Figure 6(e)** suggest that for the single integrator, the motion may slightly degrade the task performance and decrease target crossover frequency. However, the t-tests in **Figure 4** and **Figure 5(a)** show no significant difference of task performance and target crossover frequencies between C2 and C5.

4 DISCUSSION

To access the usefulness of motion feedback in flight simulators, a yaw attitude tracking experiment was conducted. This experiment focused explicitly on studying the effects of motion feedback on tracking performance, target open-loop crossover frequency and phase margin with gain, single integrator and double integrator controlled elements. The closed-loop target-to-error and disturbance-to-error frequency responses were analysed to help explain the measured task performance results and more explicitly show the potential change in the pilots' manual control behavior.

For the double integrator controlled element, the results of this experiment confirm the conclusions of previous studies [4, 5, 6, 7, 8] that the motion feedback is highly beneficial in improving tracking task performance, decreasing target crossover frequency and improving closed-loop system stability. These effects are also clearly visible from the closed-loop error frequency response analysis, where the error amplification peak is seen to reduce significantly when motion feedback is present.

For the single integrator controlled element, even though a slight decrease in the average target crossover frequency and a slightly degraded average tracking performance are observed when motion feedback is available, the effect of motion is not significant. Meanwhile, the target phase margin does not change much after motion is added, either. These may be due to the fact that, when motion is added, the error signal attenuations with respect to both target and disturbance do not change much, which suggest that the motion feedback is not utilized by the pilots for the single integrator controlled element.

For the gain controlled element, the curve of the target-to-error frequency response function moves a little bit to the left when motion feedback added. However, due to the peak of the curve also drops as it moves to the left, which may compensate the effect for which the curve moves left, the target component of the tracking error does not change much eventually. The target crossover frequency stays the same after the motion feedback is added. All of these highly indicate that the motion feedback is not utilized in the gain control tasks, either.

With the extensive analysis performed in this paper, the effects of motion feedback on key dependent variables related to pilot control – i.e., task performance, target crossover frequency and phase margin – have been evaluated. However, the changes in pilot manual control behavior were not quantified directly, by explicitly measuring the dynamics of the pilots' visual and motion feedback responses. Current ongoing work focuses on application of state-of-the-art pilot modelling techniques to the results of the experiment described in this paper. This further analysis will result in more detailed information on how exactly pilots adapt and optimize their control behavior for different controlled elements both with and without motion feedback.

5 CONCLUSIONS

A human-in-the-loop yaw attitude compensatory tracking experiment was used to evaluate the effects of simulator motion feedback on task performance, target open-loop crossover frequency and phase margin with gain, single integrator and double integrator controlled elements. For the double integrator, this experiment confirms the conclusion of previous studies that motion feedback is highly beneficial in improving tracking task performance, lowering down the target open-loop crossover frequency and improving the stability of the closed-loop system. For both the single integrator and gain controlled elements, no significant changes in tracking performance, decrease of target crossover frequency, or increase of target phase margin were observed. Thus, for high-order and low-stability dynamics as a double integrator, the motion feedback is indispensable to pilots for achieving satisfactory tracking performance. However, for more stable dynamics such as a single integrator and a gain, the motion feedback does not show similar beneficial effects. The results of the current paper suggest that the pilots' manual control behavior in moving-base flight simulators is affected by the available motion feedback for only low-stability controlled systems.

6 REFERENCES

[1] McRuer, Duane T., "Human Pilot Dynamics in Compensatory Systems, Theory Models and Experiments with Controlled Element and Forcing Function Variations," Air Force Flight Dynamics Laboratory, Wright-Patterson Air Force Base (OH), 1965.

[2] D. M. Pool, Objective Evaluation of Flight Simulator Motion Cueing Fidelity Through a Cybernetic

Approach, Delft: Delft University of Technology, Faculty of Aerospace Engineering, 2012.

[3] Zaal, Peter M. T. and Pool, Daan M. and de Bruin, Jaap and Mulder, Max and van Paassen, Marinus M., "Use of Pitch and Heave Motion Cues in a Pitch Control Task," *Journal of Guidance, Control, and Dynamics,* vol. 32, no. 2, pp. 366-377, 2009.

[4] Shirley, Richard S. and Young, Laurence R., "Motion Cues in Man-Vehicle Control -- Effects of Roll-Motion Cues on Human Operator's Behavior in Compensatory Systems with Disturbance Inputs," *IEEE Transactions on Man-Machine Systems,* vol. 9, no. 4, pp. 121-128, 1968.

[5] Stapleford, Robert L. and Peters, Richard A. and Alex, Fred R., "Experiments and a Model for Pilot Dynamics with Visual and Motion Inputs," NASA CR-1325, Hawthorne (CA), 1969.

[6] Ringland, R. F. and Stapleford, Robert L., "Motion Cue Effects on Pilot Tracking," in *Seventh Annual Conference on Manual Control*, 1971.

[7] van der Vaart, J. C., Modelling of Perception and Action in Compensatory Manual Control Tasks, Delft: Delft University of Technology, Faculty of Aerospace Engineering, 1992.

[8] Hosman, Ruud J. A. W., Pilot's Perception and Control of Aircraft Motions, Delft: Delft University of Technology, Faculty of Aerospace Engineering, 1996.

[9] Bergeron, Hugh P., "Investigation of Motion Requirements in Compensatory Control Tasks," *IEEE Transactions on Man-Machine Systems,* Vols. MMS-11, no. 2, pp. 123-125, 1970.

[10] Young, Laurence R., "Some Effects of Motion Cues on Manual Tracking," in *Second Annual NASA-University Conference on Manual Control, Massachusetts Institute of Technology*, Cambridge , 1966.

[11] Junker, Andrew M. and Replogle, Clyde R., "Motion Effects on the Human Operator in a Roll Axis Tracking Task," *Aviation, Space, and Environmental Medicine,* vol. 46, no. 6, pp. 819-822, 1975.

[12] van Paassen, Marinus M., Biophysics in Aircraft Control, A Model of the Neuromuscular System of the Pilot's Arm, Delft: Delft University of Technology, Faculty of Aerospace Engineering, 1994.

[13] Zaal, Peter M. T. and Pool, Daan M. and Chu, Q. P. and van Paassen, Marinus M. and Mulder, Max and Mulder, Jan A., "Modeling Human Multimodal Perception and Control Using Genetic Maximum Likelihood Estimation," *Journal of Guidance, Control, and Dynamics,* vol. 32, no. 4, pp. 1089-1099, 2009.

[14] T. Lu, D. M. Pool, M. M. van Paassen, M. Mulder, "The Effects of Motion Feedback on Human Operator Control Behavior with Different Controlled Elements," In preparation.

[15] Nieuwenhuizen, Frank M. and Zaal, Peter M. T. and Mulder, Max and van Paassen, Marinus M. and Mulder, Jan A., "Modeling Human Multichannel Perception and Control Using Linear Time-Invariant Models," *Journal of Guidance, Control, and Dynamics,* vol. 31, no. 4, pp. 999--1013, 2008.

[16] Damveld, Herman J. and Beerens, Gijs C. and van Paassen, Marinus M. and Mulder, Max, "Design of Forcing Functions for the Identification of Human Control Behavior," *Journal of Guidance, Control, and Dynamics,* vol. 33, no. 4, pp. 1064-1081, 2010.

[17] Jex, Henry R. and Magdaleno, R. E. and Junker, Andrew M., "Roll Tracking Effects of G-vector Tilt and Various Types of Motion Washout," in *Proceedings of the Fourteenth Annual Conference on Manual Control*, 1978.